JOBS
مجلة العلوم الأساسية
Journal of Basic Science
Print -ISSN 2306-5249
Online-ISSN 2791-3279
العدد السابع عشر
2023م /1444هـ
العدد السابع عشر
(362)- (345)

تأثير الاجهاد الثنائي، والدوران على النقل التمعجي لسائل سوتربي في قناة غير متماثلة مائلة تحتوي على وسط مسامي

أسماء عبد الحسين محمد ، لقاء زكي حمادي
جامعة بغداد/ كلية العلوم
liqqa.hummady@sc.uobaghdad.edu.iq – asmaaaa_math@csw.uobaghdad.edu.iq

المستخلص:
في هذا البحث تم دراسة تأثير الاجهاد الثنائي و متغير الدوران على التدفق التمعجي لسائل ساتيربي في قناة غير متماثلة مائلة تحتوي على وسط مسامي مع انتقال الحرارة. في وجود الدوران و الاجهاد الثنائي، تم تطوير النمذجة الرياضية باستخدام المعادلات الاساسية القائمة على نموذج سائل سوتربي. في تحليل التدفق، تم استخدام افتراضات مثل تقريب طول الموجة الطويلة وانخفاض عدد رينولدز. تم حل المعادلة غير الخطية الناتجة عدديًا باستخدام طريقة الاضطراب. تم تحليل تأثيرات المعلمات الفيزيائية المختلفة مثل معلمة الاجهاد الثنائي و رقم كراشوف و ورقم هارتمان و ورقم رينولد و رقم فرود و معلمة هال و رقم دارسي و المجال المغناطيسي ومعلمة سائل سوتربي و تحليل نقل الحرارة على توزيع السرعة و تدرج الضغط بيانياً. باستخدام برنامج ماثيماتيكا، تم حساب النتائج العددية.
الكلمات المفتاحية: التدفق التمعجي، نقل الحرارة، القناة المائلة، الوسط المسامي .

Effect of Couple-stress and Rotation on Peristaltic Transport of Sutterby Fluid in an Inclined, Asymmetric Channel Containing a Porous Medium

Asmaa A. Mohammed Liqaa Zeki Hummady
, University of Baghdad / College of Science
asmaaaa_math@csw.uobaghdad.edu.iq. , liqqa.hummady@sc.uobaghdad.edu.iq.

JOBS
مجلة العلوم الأساسية
Journal of Basic Science
Print -ISSN 2306-5249
Online-ISSN 2791-3279
العدد السابع عشر
2023م /1444هـ

Abstract:

In this paper, the effect of the couple–stress and other variables on the peristaltic flow of Sutterby fluid in an inclined asymmetric channel containing a porous medium with heat transfer is examined. In the presence of rotation and couple–stress , mathematical modeling is developed using constitutive equations based on the model of Sutterby fluid. In flow analysis, assumptions such as long wavelength approximation and low Reynolds number are used. The resulting nonlinear equation was numerically solved using the perturbation method. The effects of various physical parameters such as the couple-stress parameter, the Grashof number, the Hartmann number, the Reynold number, the Froude number, the Hall parameter, the Darcy number, the magnetic field, the Sutterby fluid parameter, and heat transfer analysis on velocity distribution and the pressure gradient are analyzed graphically. Utilizing MATHEMATICA software, numerical results were computed.
Keywords: Peristaltic flow, Heat transform, Inclined channel .

Introduction:

Peristaltic pumping is a special type of pumping when it is simple to transport a variety of complex rheological fluids from one location to another. This pumping principle is referred to as peristaltic (Mohaisen & Abedulhadi, 2022). Some examples of such physiological processes are the passage of food, chyme, and urine. Peristalsis is the driving force behind everything from worm movement to the transfer of noxious and clean fluids to the operation of finger pumps and the heart-lung machine. Damping, dispensability and tension in the vasculature play a critical part in physiological processes involving peristalsis, such as blood flow (Hayat et al., 2017). Studies of peristalsis were first introduced by (Latham, 1966; Shapiro et al., 1969). Since then, researchers have made numerous attempts to dissect the peristaltic movement of fluids and its implications in the medical and business worlds. In biological systems and industrial fluid transport, heat transfer is a fundamental principle. One of the most essential roles of the cardiovascular system is maintaining the body's temperature. Air that enters the lungs must also be tempered to the

body's temperature. This is accomplished through the use of all blood vessels. There are three methods of heat transmission; however, convection is the most relevant for fluid circulation in the human body. Human and animal bodies use convection heat transfer to release heat generated by metabolic processes into the environment (Mohaisen & Abedulhadi, 2022). In recent years, the effects of changing viscosity, heat transfer, and mass transfer on magnetohydrodynamic (MHD) peristaltic flow in an asymmetric tapering inclined channel with porous material were Examined (Kareem & Abdulhadi, 2020). For a high magnetic field like in MHD flows, hall current has significant effects. This phenomenon is widely used in a variety of fields, including the design of power generators, Hall accelerators, refrigeration coils, electric transformers, and spacecraft propulsion systems. The peristaltic transport in the presence of Hall current has been the subject of several published works. The effect of Hall current, viscosity variation, and porous medium on the peristaltic transport of viscoelastic fluid through irregular microchannels was studied (Ali, 2022). The effect of magnetohydrodynamic (MHD) on a viscous fluid generalized burgers' fluid with a gradient constant pressure and an exponentially accelerating plate, where the no-slip hypothesis between the burgers' fluid and the exponential plate is no longer applicable, were studied (Nassief & Murad, 2020). (El-Dabe et al., 2021) studied a couple stress of peristaltic transport of Sutterby micropolar nanofluid within a

symmetric channel with a powerful magnetic field and Hall currents effect. The influence of couple stress as well as rotation on the peristaltic flow of a Powell-Eyring in an inclined, tapered, and asymmetrical channel investigates by (Abdulhussein & Abdulhadi, 2022). (Hummady & Abdulhadi, 2014) have examined the effect of MHD on a peristaltic flow of Newtonian fluid with couple stress through porous media, where the assumption of no slippage between the wall and the fluid is no longer applicable.

Since (Abdulhadi & Ahmed, 2017; Sadaf et al., 2018) examined the mechanism of peristaltic transport, it has attracted the interest of numerous researchers. Viscous liquids are less prevalent in industrial and physiological processes than non-Newtonian fluids. Shampoo, ketchup, lubricants, paints, and blood are all examples of non-Newtonian substances found in nature.

JOBS مجلة العلوم الأساسية
Journal of Basic Science
Print -ISSN 2306-5249
Online-ISSN 2791-3279
العدد السابع عشر
2023م /1444هـ

Among that, Sutterby liquid (Sutterby, 1966) is one of the materials that characterize ionic high polymer solutions. Convection and Hall current were used to simulate the MHD peristaltic transport of a Sutterby nanofluid (Hayat et al., 2021). Waveform motion of non-Newtonian fluids through porous channels is discussed (Alshareef, 2020; Kalyani & MVVNL, 2021), where the effects of rotation and an inclined MHD are considered. Magnetohydrodynamic (MHD) for Williamson fluid with variable temperatures and variable concentrations in a slanted channel with variable viscosity has been investigated (Khudair & Dwail, 2021). The effects of radiation and convection in a Sutterby fluid are discussed (Ahmad et al., 2018). In Ramesh (Ramesh & Prakash, 2019), electroosmotic peristaltic transport of Sutterby nanofluids is investigated. The peristaltic flow of a Sutterby liquid in an inclined channel was investigated (Atlas et al., 2020 .(

In this paper, the study will look at the effects of rotation on heat transfer for peristaltic transport in an inclined asymmetric channel with a porous medium. This will be done by using different values of the parameters of rotation, amplitude wave, and channel taper, as well as different values of the Grashof number, the Hartmann number, the Reynold number, the Froude number, the Hall parameter, the Darcy number, the magnetic field, the Sutterby fluid parameter, and heat transfer analysis, based on the changes in velocity and pressure gradient.

A mathematical formulation for asymmetric flow

Consider the peristaltic transport of an incompressible Sutterby fluid through a two-dimensional asymmetric conduit that has a width of (d^'+d). whereas motion is constant within a coordinate system pumped at wave speed (c) in the wave framer $(\bar{X}, \bar{Y})$.

The geometry of a wall's structure is described as:

$$\overline{h_1}(\bar{x},\bar{t}) = d - a_1 \sin\left[\frac{2\pi}{\lambda}(\bar{X} - c\bar{t})\right] \quad 1$$

$$\overline{h_2}(\bar{x},\bar{t}) = -d' - a_2 \sin\left[\frac{2\pi}{\lambda}(\bar{X} - c\bar{t}) + \Phi\right] \quad 2$$

In which $\overline{h_1}(\bar{x},\bar{t})$, $\overline{h_2}(\bar{x},\bar{t})$ are the lower and upper wall respectively, (d, d') indicates the channel width, (a_1, a_2) are the wave's amplitudes, (λ) represents the wavelength, (c) is the speed of a wave, (Φ) varies in the range

JOBS مجلة العلوم الأساسية Journal of Basic Science
Print -ISSN 2306-5249
Online-ISSN 2791-3279
العدد السابع عشر
1444/ 2023هـ

$(0 \leq \Phi \leq \pi)$, when the value of $\Phi = 0$ the channel is symmetric with waves out of phase and $\Phi = \pi$ waves are in phase the rectangular coordinates has been designed in such a method that $\bar{X} - axis$ is along the path that waves use for propagation and $\bar{Y} - axis$ perpendicular to $\bar{X}$, $\bar{t}$ represents the time. Further a_1, a_2, d, d' and Φ satisfy the following condition:

$$a_1^2 + a_2^2 + 2a_1a_2 \cos\Phi \leq (d + d')^2 \quad (3)$$

Basic equation

The additional stress tensor for the Sutterby model is determined by (Ramesh & Prakash, 2019):

$$\bar{S} = \frac{\mu}{2}\left[\frac{\sinh^{-1}(n\dot{\gamma})}{n\dot{\gamma}}\right]^{m^*} A_1 \quad (4)$$

$$\dot{\gamma} = \sqrt{\frac{1}{2}\text{tras}(A_1)^2} \quad (5)$$

$$A_1 = \nabla\bar{V} + (\nabla\bar{V})^T \quad (6)$$

Where $\bar{S}$ denotes the stress of the extra tensor, n, and m^* represents the material constants of the Sutterby fluid, $\nabla = (\partial\bar{X}, \partial\bar{Y}, 0)$ is the gradient vector, μ represents the dynamic viscosity and A_1 represents the first Rivilin–Ericksen tensor. The phrase $\sinh^{-1}$ is approximately equivalent to

$$\sinh^{-1}\left(\frac{\dot{\gamma}}{n}\right) = \frac{\dot{\gamma}}{n} - \frac{\dot{\gamma}^3}{6n^3} \quad , \left|\frac{\dot{\gamma}^5}{6n^5}\right| \ll 1 \quad (7)$$

The constituents of the extra stress tensor of Sutterby defined by Eq.**4** are listed below:

$$\bar{S}_{\bar{X}\bar{X}} = \frac{\mu}{2}[1 - \frac{mn^2}{6}\left(2\bar{U}_{\bar{X}}{}^2 + (\bar{V}_{\bar{X}} + \bar{U}_{\bar{Y}})^2 + 2\bar{V}_Y{}^2\right)]2\bar{U}_{\bar{X}} \quad (8)$$

$$\bar{S}_{\bar{X}\bar{Y}} = \frac{\mu}{2}\left[1 - \frac{mn^2}{6}\left(2\bar{U}_{\bar{X}}{}^2 + (\bar{V}_{\bar{X}} + \bar{U}_{\bar{Y}})^2 + 2\bar{V}_Y{}^2\right)\right](\bar{U}_{\bar{X}} + \bar{V}_{\bar{Y}}) \quad (9)$$

$$\bar{S}_{\bar{Y}\bar{Y}} = \frac{\mu}{2}\left[1 - \frac{mn^2}{6}\left(2\bar{U}_{\bar{X}}{}^2 + (\bar{V}_{\bar{X}} + \bar{U}_{\bar{Y}})^2 + 2\bar{V}_Y{}^2\right)\right]2\bar{V}_{\bar{Y}} \quad (10)$$

The governing equations

The flow is controlled by three coupled nonlinear partial differentials of continuity, momentum, and energy, the governing equations in frame $(\bar{X}, \bar{Y})$ can be written as follows:

JOBS مجلة العلوم الأساسية Journal of Basic Science
Print -ISSN 2306-5249
Online-ISSN 2791-3279
العدد السابع عشر
1444/ م2023هـ

$$\frac{\partial \bar{U}}{\partial \bar{X}} + \frac{\partial \bar{V}}{\partial \bar{Y}} = 0 \quad (11)$$

$$\rho\left(\frac{\partial \bar{U}}{\partial \bar{t}} + \bar{U}\frac{\partial \bar{U}}{\partial \bar{X}} + \bar{V}\frac{\partial \bar{U}}{\partial \bar{Y}}\right) - \rho\Omega\left(\Omega\bar{U} + 2\frac{\partial \bar{V}}{\partial \bar{t}}\right) = -\frac{\partial \bar{P}}{\partial \bar{X}} + \frac{\partial \bar{S}_{\bar{X}\bar{X}}}{\partial \bar{X}} + \frac{\partial \bar{S}_{\bar{X}\bar{Y}}}{\partial \bar{Y}} - \frac{\sigma {B_0}^2}{(1+m^2)}(\bar{U} - m\bar{V}) + g\rho\beta_T(T - T_0) - \frac{\mu}{k_0}\bar{U} - \mu_1\nabla^4\bar{U} + \rho g sin(\alpha 1) \quad (12)$$

$$\rho\left(\frac{\partial \bar{V}}{\partial \bar{t}} + \bar{U}\frac{\partial \bar{V}}{\partial \bar{X}} + \bar{V}\frac{\partial \bar{V}}{\partial \bar{Y}}\right) - \rho\Omega\left(\Omega\bar{V} - 2\frac{\partial \bar{U}}{\partial \bar{t}}\right) = -\frac{\partial \bar{P}}{\partial \bar{Y}} + \frac{\partial \bar{S}_{\bar{X}\bar{Y}}}{\partial \bar{X}} + \frac{\partial \bar{S}_{\bar{Y}\bar{Y}}}{\partial \bar{Y}} - \frac{\sigma {B_0}^2}{(1+m^2)}(\bar{V} + m\bar{U}) - \frac{\mu}{k_0}\bar{V} - \mu_1\nabla^4\bar{V} + \rho g cos(\alpha 1) \quad (13)$$

$$\rho C_P\left(\frac{\partial}{\partial \bar{t}} + \bar{U}\frac{\partial}{\partial \bar{X}} + \bar{V}\frac{\partial}{\partial \bar{Y}}\right)\bar{T} = \kappa\left(\frac{\partial^2}{\partial \bar{t}^2} + \frac{\partial^2}{\partial \bar{X}^2} + \frac{\partial^2}{\partial \bar{Y}^2}\right)\bar{T} + \varphi_0 \quad (14)$$

Where ρ is the fluid density, $(\bar{U}, \bar{V})$ the velocity components, $\bar{P}$ represents the hydrodynamic pressure, $\bar{S}_{\bar{X}\bar{X}}, \bar{S}_{\bar{X}\bar{Y}}$, and $\bar{S}_{\bar{Y}\bar{Y}}$ are the constituents of the extra stress tensor $\bar{S}$. σ is the electrical conductivity, φ_0 is the steady heat addition/absorption, B_0 is an applied magnetic field, β_T is the thermal expansion coefficient, g is the gravitational acceleration, μ_1 is a constant linked to the couple stress , and Ω represents the rotation. The specific heat is denoted by C_P, $\alpha 1$ is the channel's angle of inclination with respect to the horizontal axis, k_0 material constant, the thermal conductivity by k, and the temperature by $\bar{T}$. And

$$\nabla^2 = \frac{\partial^2}{\partial \bar{X}^2} + \frac{\partial^2}{\partial \bar{Y}^2}, \nabla^4 = \frac{\partial^4}{\partial \bar{X}^4} + 2\frac{\partial^4}{\partial \bar{X}^2 \partial \bar{Y}^2} + \frac{\partial^4}{\partial \bar{Y}^4}$$

Peristaltic movement in reality is an unsteady behavior, but it can be considered to be steady via the change from the experimental frame (fixed frame) $(\bar{X}, \bar{Y})$ to the wave frame (move frame) $(\bar{x}, \bar{y})$. The following transformations establish the link between coordinates, velocities, and pressure in laboratory frame $(\bar{X}, \bar{Y})$ to wave frame $(\bar{x}, \bar{y})$:

$$\bar{x} = \bar{X} - c\bar{t}\ , \bar{y} = \bar{Y}\ , \bar{u} = \bar{U} - c\ , \bar{v} = \bar{V}\ , \bar{p}(\bar{x}, \bar{y}) = \bar{P}(\bar{X}, \bar{Y}, \bar{t}) \quad (15)$$

Where $\bar{u}$ and $\bar{v}$ represent the components of velocity, and $\bar{p}$ denotes the pressure in the wave frame. Now, Eqs.**15** will be substituted into Eqs.**1**,**2** and Eq.**8**-Eq.**14** and then normalize the equation that is produced by doing so by utilizing the non-dimensional quantities that are listed below:

JOBS مجلة العلوم الأساسية
Journal of Basic Science
Print -ISSN 2306-5249
Online-ISSN 2791-3279
العدد السابع عشر
1444/ م2023هـ

$$x=\frac{1}{\lambda}\bar{x},\ y=\frac{1}{d}\bar{y},\ u=\frac{1}{c}\bar{u},\ v=\frac{1}{c}\bar{v},\ p=\frac{d^2}{\lambda\,\mu\,c}\bar{p},\ t=\frac{c}{\lambda}\bar{t},\ h_1=\frac{1}{d}\overline{h_1},$$
$$h_2=\frac{1}{d}\overline{h_2},\quad \delta=\frac{d}{\lambda},\quad Re=\frac{\rho\,c\,d}{\mu},\quad \bar{T}=T-T_0,\quad \theta=\frac{T-T_0}{T_1-T_0},\ S_{ij}= \qquad 16$$
$$\frac{d}{\mu\,c}\bar{S}_{\bar{I}\,\bar{J}},\ Gr=\frac{g\beta_T(T-T_0)d^2}{\mu c},\ Pr=\frac{\mu c_p}{k},\ \mathrm{Fr}=\frac{c^2}{gd},\ Da=\frac{k_0}{d^2},\ \alpha=d\sqrt{\frac{\mu}{\mu_1}}$$

Where, (δ) represents the wave number, $(h_1)\ and\ (h_2)$ are the nondimensional upper and lower wall surface respectively, (Re) represents the Reynolds number, (Pr) represents the Prandtl number, (Gr) represents the Grashof number, (Fr) represents the Froude number, (M) represents the Hartman number, (Da) represents Darcy number, (Φ) represents the face difference,(A) represents the parameter of Sutterby liquid, (α) represents the couple stress parameter, and $(T_0)\ and\ (T_1)$ are the wall temperatures at the top and bottom, respectively. Then, in view of Eqs.**16**, Eq.1,2, and **8-14** take the form :

$$h_1(x)\ =\ 1+a\ sin \qquad 17$$
$$h_2(x)=-d_1-b\ \ sin\ (x+\Phi) \qquad 18$$
$$\delta\frac{\partial u}{\partial x}+\frac{\partial v}{\partial y}=0 \qquad 19$$
$$Re\left(\delta\frac{\partial u}{\partial t}+\delta u\frac{\partial u}{\partial x}+v\frac{\partial u}{\partial y}\right)-\frac{\rho d^2}{\mu}\Omega\ \left(\Omega u\ +2\delta\frac{\partial v}{\partial t}\right)=\ -\frac{\partial p}{\partial x}+$$
$$\delta\frac{\partial S_{xx}}{\partial x}+\frac{\partial \mathrm{S_{xy}}}{\partial y}-\frac{\sigma {B_0}^2}{(1+m^2)}(u-mv)+\ Gr\ \theta-\frac{1}{Da}u-\frac{1}{\alpha^2}(\delta^4\frac{\partial^4 u}{\partial x^4}+ \qquad 20$$
$$2\delta^2\frac{\partial^4 u}{\partial x^2\partial y^2}+\frac{\partial^4 u}{\partial y^4})+\frac{Re}{Fr}\sin(\alpha 1)$$
$$Re\delta\left(\delta\frac{\partial v}{\partial t}+\delta u\frac{\partial v}{\partial x}+v\frac{\partial v}{\partial y}\right)-Re\frac{d}{c}\Omega\ \left(\Omega\delta v-2\delta^2\frac{\partial u}{\partial t}\right)=\ -\frac{\partial p}{\partial y}+$$
$$\delta^2\frac{\partial S_{xy}}{\partial x}+\delta\frac{\partial S_{yy}}{\partial y}-\frac{\sigma {B_0}^2}{(1+m^2)}\frac{d^2}{\mu}\delta(v+mu)-\frac{1}{Da}\delta v-\frac{1}{\alpha^2}\left(\delta^5\frac{\partial^4 v}{\partial x^4}+ \qquad 21$$
$$2\delta^3\frac{\partial^4 v}{\partial x^2\partial y^2}+\delta\frac{\partial^4 v}{\partial y^4}\right)+\frac{Re}{Fr}\cos(\alpha 1)$$
$$RePr\delta\left(\frac{\partial}{\partial t}+u\frac{\partial}{\partial x}+v\frac{\partial}{\partial y}\right)\theta=\left(\delta^2\frac{c^2\partial^2}{\partial t^2}+\delta^2\frac{\partial^2}{\partial x^2}+\frac{\partial^2}{\partial y^2}\right)\theta+B \qquad 22$$

Introduction to fluid flow (ψ) through a relationship:

$$u=\psi_y\ ,v=-\delta\psi_x \qquad 23$$

Substituted Eqs.**23** in Eq.**19**-Eq.**22** respectively,

JOBS مجلة العلوم الأساسية Journal of Basic Science
Print -ISSN 2306-5249
Online-ISSN 2791-3279
العدد السابع عشر
1444/ م2023هـ

$$\delta\frac{\partial\psi_y}{\partial x}-\delta\frac{\partial\psi_x}{\partial y}=0 \quad (24)$$

$$Re\left(\delta\frac{\partial\psi_y}{\partial t}+\delta\psi_y\frac{\partial\psi_y}{\partial x}-\delta\psi_x\frac{\partial\psi_y}{\partial y}\right)-\frac{\rho d^2}{\mu}\Omega\left(\Omega\psi_y-2\delta^2\frac{\partial\psi_x}{\partial t}\right)=$$
$$-\frac{\partial p}{\partial x}+\delta\frac{\partial S_{xx}}{\partial x}+\frac{\partial S_{xy}}{\partial y}-\frac{\sigma {B_0}^2}{(1+m^2)}(\psi_y+m\delta\psi_x)+\mathrm{Gr}\,\theta-\frac{1}{Da}\psi_y- \quad (25)$$
$$\frac{1}{\alpha^2}(\delta^4\frac{\partial^4\psi_y}{\partial x^4}+2\delta^2\frac{\partial^4\psi_y}{\partial x^2\partial y^2}+\frac{\partial^4\psi_y}{\partial y^4})+\frac{Re}{Fr}\sin(\alpha 1)$$

$$Re\delta\left(-\delta^2\frac{\partial\psi_x}{\partial t}-\delta^2\psi_y\frac{\partial\psi_x}{\partial x}-\delta^2\psi_x\frac{\partial\psi_x}{\partial y}\right)-Re\frac{d}{c}\Omega\left(-\Omega\delta^2\psi_x-\right.$$
$$\left.2\delta^2\frac{\partial\psi_y}{\partial t}\right)=-\frac{\partial p}{\partial y}+\delta^2\frac{\partial S_{xy}}{\partial x}+\delta\frac{\partial S_{yy}}{\partial y}+\frac{\sigma {B_0}^2}{(1+m^2)}\frac{d^2}{\mu}\delta(-\delta\psi_x+ \quad (26)$$
$$m\psi_y)+\frac{1}{Da}\delta\psi_x-\frac{1}{\alpha^2}(-\delta^6\frac{\partial^4\psi_x}{\partial x^4}-2\delta^4\frac{\partial^4\psi_x}{\partial x^2\partial y^2}-\delta^2\frac{\partial^4\psi_x}{\partial y^4})+$$
$$\frac{Re}{Fr}\cos(\alpha 1)$$

$$RePr\delta\left(\frac{\partial}{\partial t}+\psi_y\frac{\partial}{\partial x}-\delta\psi_x\frac{\partial}{\partial y}\right)\theta=\left(\delta^2\frac{c^2\partial^2}{\partial t^2}+\delta^2\frac{\partial^2}{\partial x^2}+\frac{\partial^2}{\partial y^2}\right)\theta+B \quad (27)$$

When (δ <<1), the equations from Eqs.**25-27** become in the form :

$$-\frac{\rho d^2}{\mu}\Omega^2\psi_y=-\frac{\partial p}{\partial x}+\frac{\partial S_{xy}}{\partial y}-(\frac{M^2}{1+m^2}+\frac{1}{Da})\psi_y+Gr\,\theta-\frac{1}{\alpha^2}\frac{\partial^5\psi}{\partial y^5}+ \quad (28)$$
$$\frac{Re}{Fr}\sin(\alpha 1)$$

$$-\frac{\partial p}{\partial y}=0 \quad (29)$$

$$\frac{\partial^2\theta}{\partial y^2}+\mathrm{B}=0 \quad (30)$$

While an additional stress tensor component takes the following form:

$$S_{xy}=\frac{1}{2}\frac{\partial^2\psi}{\partial y^2}-A\left(\frac{\partial^2\psi}{\partial y^2}\right)^3, S_{xx}=0, S_{yy}=0 \quad (31)$$

Where $M=\sqrt{\frac{\sigma}{\mu}}B_0 d$ the Hartman number, $A=\frac{\boldsymbol{mb^2c^2}}{\boldsymbol{6d^2}}$ the Sutterby liquid parameter and $B=\frac{d^2\varphi_0}{k(T_1-T_0)}$ the constant heat radiation

If Eq.**31** is substituted into Eq.**28** and the derivative with respect to y is taken, the following equation is obtained:

$$\frac{2}{\alpha^2}\frac{\partial^6\psi}{\partial y^6}-\frac{\partial^4\psi}{\partial y^4}\left[1-3A\left(\frac{\partial^2\psi}{\partial y^2}\right)^2\right]+6A\frac{\partial^2\psi}{\partial y^2}\left(\frac{\partial^3\psi}{\partial y^3}\right)^2-2\left(\frac{\rho d^2}{\mu}\Omega^2-\right. \quad (32)$$
$$\left.\frac{M^2}{m^2+1}-\frac{1}{Da}\right)\frac{\partial^2\psi}{\partial y^2}-2Gr\frac{\partial\theta}{\partial y}=0$$

$$\frac{\partial^2\theta}{\partial y^2}+B=0 \quad (33)$$

JOBS مجلة العلوم الأساسية
Journal of Basic Science
Print -ISSN 2306-5249
Online-ISSN 2791-3279
العدد السابع عشر
2023م /1444هـ

In wave frames, the dimensionless boundary conditions

$$\frac{\partial\psi}{\partial y}+\beta\frac{\partial^2\psi}{\partial y^2}=-1,\psi=\frac{F}{2},\frac{\partial^3\psi}{\partial y^3}=0 \quad at\ y=h_1 \qquad 34$$

$$\frac{\partial\psi}{\partial y}-\beta\frac{\partial^2\psi}{\partial y^2}=-1,\psi=-\frac{F}{2},\frac{\partial^3\psi}{\partial y^3}=0 \quad at\ y=h_2 \qquad 35$$

$$\theta=0\ at\ y=h_1\ ,\theta=1\ \ at\ y=h_2 \qquad 36$$

Where F is just the flow rate, which is dimensionless in time in the frame of the wave. It is associated with the form that has no dimensions' temporal flow rate *Q1* in the experimental frame via the expression:

$$Q_1=F+1+d \qquad 37$$

as a, b, Φ and d achieve Eq.**3**:

$$a^2+b^2+2abcos(\Phi)\leq(1+d_1)^2 \qquad 38$$

Initially, the nonlinear equation Eq.**33** is solved by integrating and substituting the boundary conditions Eq.**36**, and then the solution to Eq.**37** is obtained :

$$\theta=-\frac{-2h_1+h_1^2h_2B-h_1h_2^2B}{2(h_1-h_2)}-\frac{(2-h_1^2B+h_2^2B)y}{2(h_1-h_2)}-\frac{By^2}{2} \qquad 39$$

By differentiating Eq.**39** with respect to y and substituting it into Eq.**32**, obtaining the following nonlinear equation:

$$\frac{2}{\alpha^2}\frac{\partial^6\psi}{\partial y^6}-\frac{\partial^4\psi}{\partial y^4}\left[1-3A\left(\frac{\partial^2\psi}{\partial y^2}\right)^2\right]+6A\frac{\partial^2\psi}{\partial y^2}\left(\frac{\partial^3\psi}{\partial y^3}\right)^2-2\left(\frac{\rho d^2}{\mu}\Omega^2-\frac{M^2}{m^2+1}-\frac{1}{Da}\right)\frac{\partial^2\psi}{\partial y^2}+2Gr\left(-\frac{(2-h_1^2B+h_2^2B)}{2(h_1-h_2)}-By\right)=0 \qquad 40$$

Solution of the problem

It is not possible to that construct a solution in closed form for each and every one of the arbitrary parameters involved in Eq.**40**, as it is highly non-linear and convoluted. Therefore, the perturbation approach is used to get the answer. The solution was expanded to include perturbation (Abdulla & Hummady, 2021) :

$$\psi=\psi_0+A\psi_1+o(A^2) \qquad 41$$

And by substituting the expressions Eq.**41** into Eq.**40**, along with the boundary conditions Eq.**34** and Eq.**35** and equating the coefficients of similar powers of A, The following system of equations is obtained:

1. Zeroth order system

When such terms of order (A) in a zero-order system are negligible, the result is

JOBS مجلة العلوم الأساسية Journal of Basic Science
Print -ISSN 2306-5249
Online-ISSN 2791-3279
العدد السابع عشر
2023م /1444هـ

$$\frac{2}{\alpha^2}\frac{\partial^6\psi_0}{\partial y^6}-\frac{\partial^4\psi_0}{\partial y^4}-\zeta\frac{\partial^2\psi_0}{\partial y^2}+\gamma y-\eta=0 \quad (42)$$

Where $\zeta=2(\frac{\rho d^2}{\mu}\Omega^2-\frac{1}{Da}-\frac{M^2}{m^2+1})$

$\gamma=2GrB$

And $\eta=Gr[B(h_1+h_2)-\frac{2}{h_1-h_2}]$

Such that

$$\frac{\partial\psi_0}{\partial y}+\beta_1\frac{\partial^2\psi_0}{\partial y^2}=-1,\psi_0=\frac{F_0}{2},\frac{\partial^3\psi_0}{\partial y^3}=0 \quad at\ y=h_1 \quad (43)$$

and

$$\frac{\partial\psi_0}{\partial y}-\beta_1\frac{\partial^2\psi_0}{\partial y^2}=-1,\psi_0=-\frac{F_0}{2},\frac{\partial^3\psi_0}{\partial y^3}=0 \quad at\ y=h_2 \quad (44)$$

First order system

$$\frac{2}{\alpha^2}\frac{\partial^6\psi_1}{\partial y^6}-\frac{\partial^4\psi_1}{\partial y^4}-\zeta\frac{\partial^2\psi_1}{\partial y^2}+3\frac{\partial^4\psi_0}{\partial y^4}\left(\frac{\partial^2\psi_0}{\partial y^2}\right)^2+6\frac{\partial^2\psi_0}{\partial y^2}\left(\frac{\partial^3\psi_0}{\partial y^3}\right)^2+\gamma y-\eta=0 \quad (45)$$

$$\frac{\partial\psi_1}{\partial y}+\beta_1\frac{\partial^2\psi_1}{\partial y^2}=-1,\psi_1=\frac{F_1}{2},\frac{\partial^3\psi_1}{\partial y^3}=0 \quad at\ y=h_1 \quad (46)$$

and

$$\frac{\partial\psi_1}{\partial y}-\beta_1\frac{\partial^2\psi_1}{\partial y^2}=-1,\psi_1=-\frac{F_1}{2},\frac{\partial^3\psi_1}{\partial y^3}=0 \quad at\ y=h_2 \quad (47)$$

Solving the relevant zeroth-order and first-order systems yields the final stream function equation.

$$\psi=\psi_0+A\psi_1 \quad (48)$$

Results and discussions:

This section consists of two subsections. Using MATHEMATICA, the velocity distribution is depicted in the first and the pressure gradient is presented in the second.

1. Velocity distribution u:

For changing values of u, reflects the variation in axial velocity throughout the channel. The influence different values of on axial velocity u are introduced in .The (**Figure 1-Figure 9**) show the effect of changing the values of $\Omega, M, Gr, m,\ A,\ \alpha, \phi, B, Da\ and\ \phi$ on the axial velocity u. In **Figure**

JOBS مجلة العلوم الأساسية
Journal of Basic Science
Print -ISSN 2306-5249
Online-ISSN 2791-3279
العدد السابع عشر
1444/ م2023هـ

1,we can see that as the rotation (Ω) goes up, the axial velocity has no effect. **Figure 2** shows that as the Hartmann number (*M*) goes up, the axial velocity also has no effect. As illustrated in **Figure 3**, the axial velocity reduces near the left wall of the channel and middle of the channel from the right side as the thermal Grashof number (*Gr*) increases, while it rises near the right wall of the channel and middle of the channel from the left side. As shown in **Figure 4**, increasing the value of the Hall parameter (*m*) doesn't change the axial speed. As illustrated in **Figure 5**, the axial velocity is increased in the middle of the channel as the fluid parameter (*A*) increases, whereas it decreases near the channel walls. **Figure 6** shows that raising the couple stress parameter (α) doesn't change the axial speed. As seen in **Figure 7**, as the constant heat radiation (*B*) grows, the axial velocity doesn't change. **Figure 8** shows that the axial velocity doesn't change as the Darcy number (*Da*) increases. **Figure 9** demonstrates that, as the face difference (ϕ) increases, the axial velocity decreases along the left side and the near right side of the channel wall while it increases near the middle of the channel from the right side.

2. Pressure gradient dp/dx:

Graphically, the influence that relevant parameters $\Omega, M, Gr, m, A, \alpha, Re, Fr, B, Da, \phi, and\ \alpha 1$ have on the pressure gradient dp/dx can be seen in **Figure 10-Figure 21**. As seen in **Figure 10**, increasing the rotation (Ω) has no effect in pressure gradient. **Figure 11** illustrates how increasing values of the Hartmann number (*M*) are doesn't change in pressure gradient. Increasing the thermal Grashof number (*Gr*) increases the pressure gradient along the channel, as depicted in **Figure 12**. **Figure 13** shows that the Hall parameter value (*m*) goes up, the pressure gradient doesn't change. **Figure 14** shows that the pressure gradient rises in the middle of the channel while it decreases in near the channel wall as the value of a fluid parameter (*A*) increases. **Figure 15** shows that as raising the couple stress parameter (α) results increases in the pressure gradient. In **Figure 16**, the pressure gradient increases with the increasing Reynold number (*Re*). As shown in **Figure 17**, increasing the value of the Froude number (*Fr*) leads to a little decreases in the pressure gradient. **Figure 18** shows that as the constant heat radiation (*B*) goes up, the pressure gradient has little rises. The pressure gradient doesn't

JOBS
مجلة العلوم الأساسية
Journal of Basic Science
Print -ISSN 2306-5249
Online-ISSN 2791-3279
العدد السابع عشر
2023م /1444هـ

change with the increasing of the Darcy number (Da) as clear in **Figure 19**. **Figure 20** displays, that the pressure gradient rises along the left wall as the face difference (ϕ) increases whereas reduce along the right side of the channel. **Figure 21**, shows that the pressure gradient has little decreasing with increasing of the channel's angle of inclination with respect to the horizontal axis ($\alpha 1$).

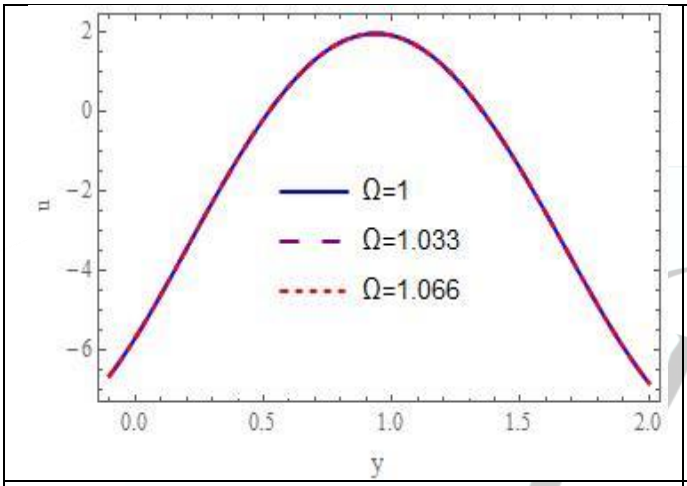

Figure 1: Velocity and variation for different of Ω when $M = 0.99, \mathrm{Gr} = 0.5, m = 0.05, A = 3, \alpha = 2.5, B = 1, \mathrm{Da} = 6, \phi = 2.4$

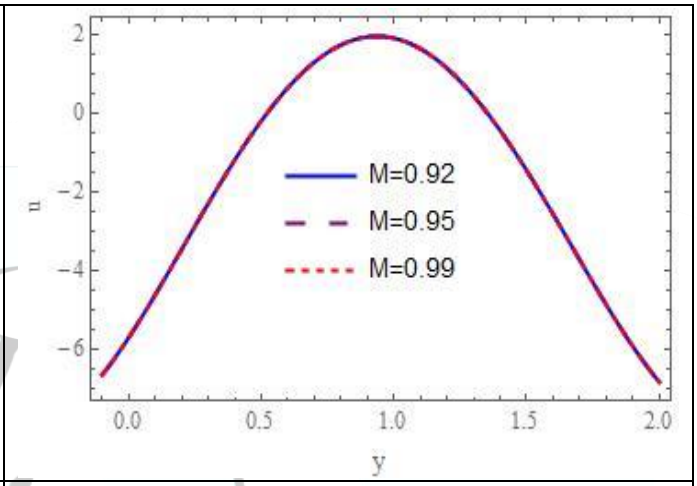

Figure 2: Velocity and variation for different of M when $\Omega = 1, \mathrm{Gr} = 0.5, m = 0.05, A = 3, \alpha = 2.5, B = 1, \mathrm{Da} = 6, \phi = 2.4$

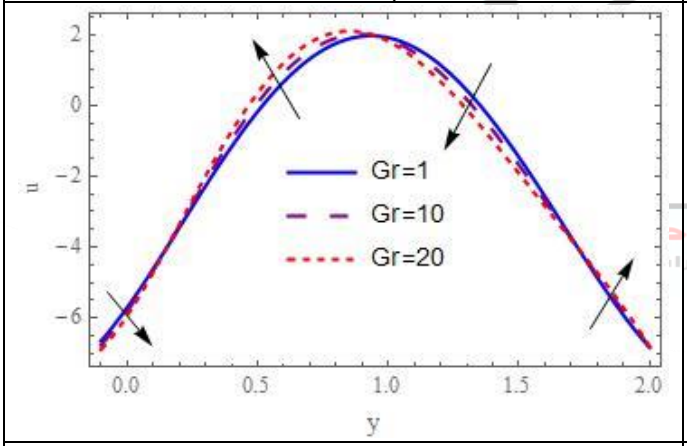

Figure 3: Velocity and variation for different of Gr when $\Omega = 1, \mathrm{M} = 0.99, m = 0.05, A = 3, \alpha = 2.5, B = 1, \mathrm{Da} = 6, \phi = 2.4$

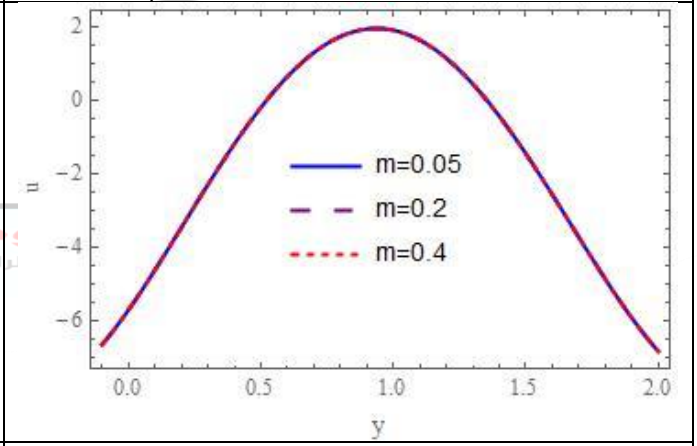

Figure 4: Velocity and variation for different of m when $\Omega = 1, \mathrm{M} = 0.9, \mathrm{Gr} = 0.5, A = 3, \alpha = 2.5, B = 1, \mathrm{Da} = 6, \phi = 2.4$

JOBS
مجلة العلوم الأساسية
Journal of Basic Science
Print -ISSN 2306-5249
Online-ISSN 2791-3279
العدد السابع عشر
2023م /1444هـ

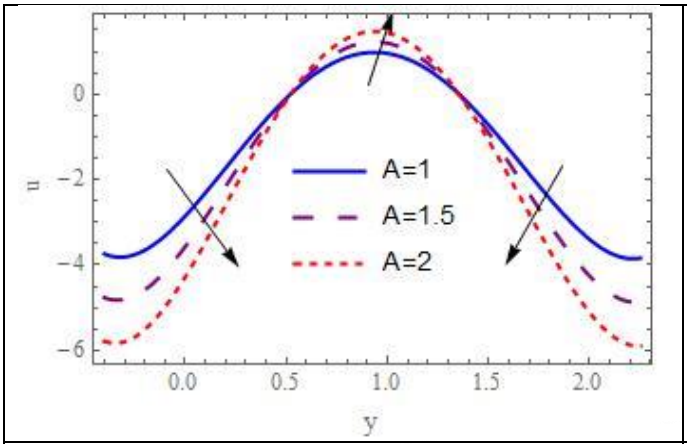

Figure 5: Velocity and variation for different of A when $\Omega = 1, \mathrm{M} = 0.9, \mathrm{Gr} = 0.5, m = 0.05, \alpha = 2.5, B = 1, \mathrm{Da} = 6, \phi = 2.4$

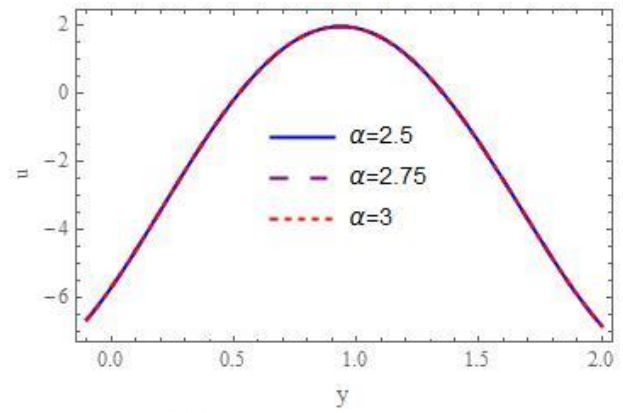

Figure 6: Velocity and variation for different of α when $\Omega = 1, \mathrm{M} = 0.9, \mathrm{Gr} = 0.5, m = 0.05, A = 3, B = 1, \mathrm{Da} = 6, \phi = 2.4$

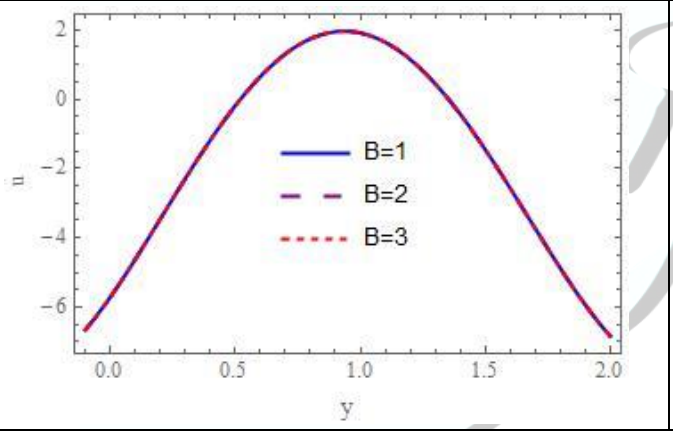

Figure 7: Velocity and variation for different of B when $\Omega = 1, \mathrm{M} = 0.9, \mathrm{Gr} = 0.5, m = 0.05, A = 3, \alpha = 2.5, \mathrm{Da} = 6, \phi = 2.41$

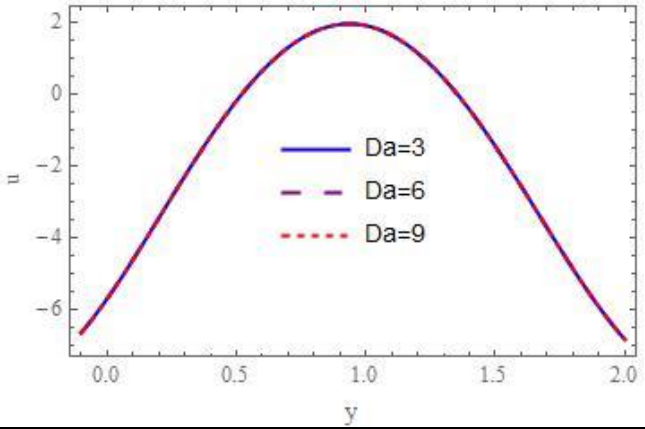

Figure 8: Velocity and variation for different of Da when $\Omega = 1, \mathrm{M} = 0.9, \mathrm{Gr} = 0.5, m = 0.05, A = 3, \alpha = 2.5, \mathrm{B} = 1, \phi = 2.4$

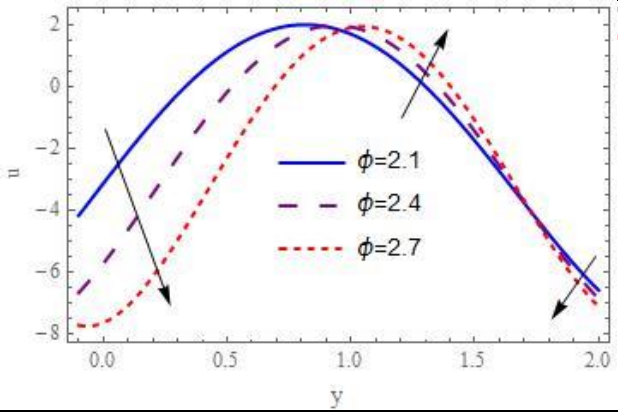

Figure 9: Velocity and variation for different of ϕ when $\Omega = 1, \mathrm{M} = 0.9, \mathrm{Gr} = 0.5, m = 0.05, A = 3, \alpha = 2.5, \mathrm{B} = 1, Da = 6$

JOBS
مجلة العلوم الأساسية
Journal of Basic Science
Print -ISSN 2306-5249
Online-ISSN 2791-3279
العدد السابع عشر
2023م /1444هـ

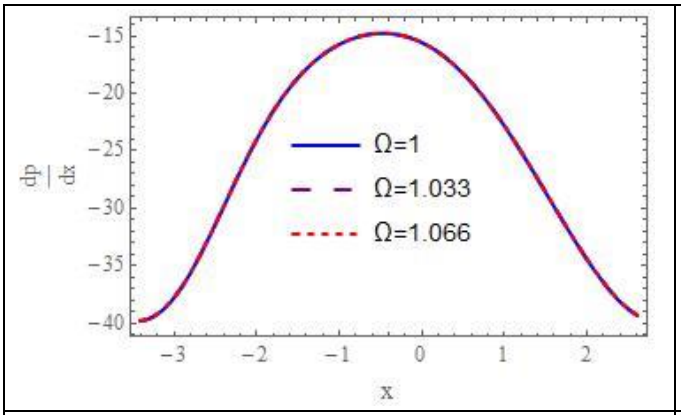

Figure 10: Pressure gradient and variation for different of Ω when $M = 0.99, \mathrm{Gr} = 0.5, m = 0.05, A = 0.05, \alpha = 2.5, \mathrm{Re} = 0.4, \mathrm{Fr} = 1, B = 1, \mathrm{Da} = 6, \phi = 2.4, \alpha 1 = 2.5$

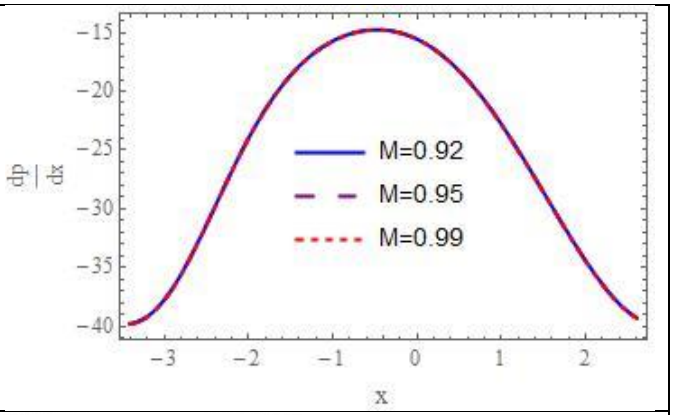

Figure 11: Pressure gradient and variation for different of M when $\Omega = 1, \mathrm{Gr} = 0.5, m = 0.05, A = 0.05, \alpha = 2.5, \mathrm{Re} = 0.4, \mathrm{Fr} = 1, B = 1, \mathrm{Da} = 6, \phi = 2.4, \alpha 1 = 2.5$

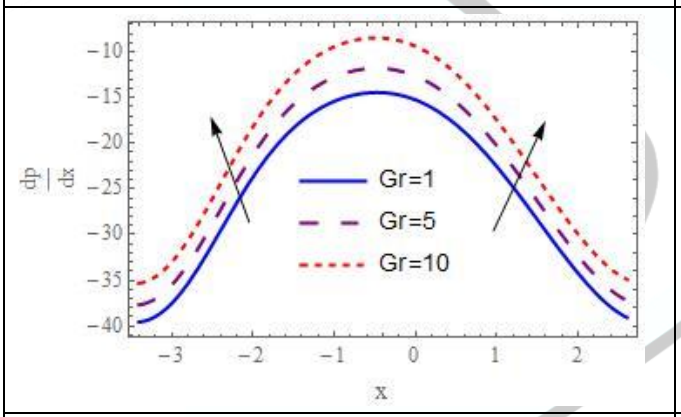

Figure 12: Pressure gradient and variation for different of Gr when $\Omega = 1, \mathrm{M} = 0.99, m = 0.05, A = 0.05, \alpha = 2.5, \mathrm{Re} = 0.4, \mathrm{Fr} = 1, B = 1, \mathrm{Da} = 6, \phi = 2.4, \alpha 1 = 2.5$

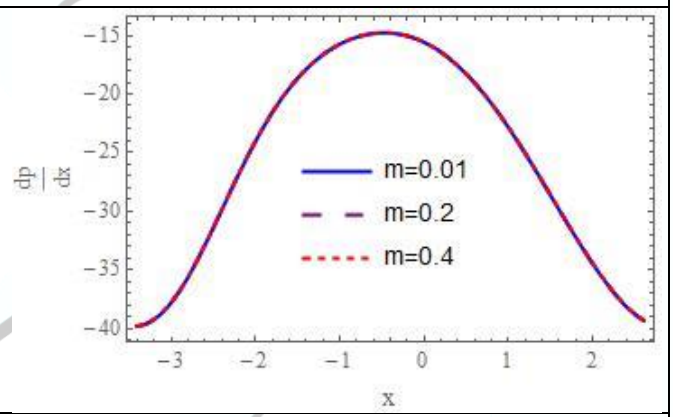

Figure 13: Pressure gradient and variation for different of m when $\Omega = 1, \mathrm{M} = 0.99, Gr = 0.5, A = 0.05, \alpha = 2.5, \mathrm{Re} = 0.4, \mathrm{Fr} = 1, B = 1, \mathrm{Da} = 6, \phi = 2.4, \alpha 1 = 2.5$

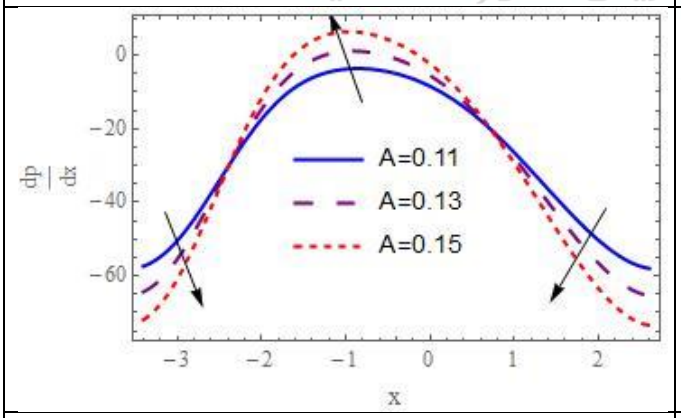

Figure 14: Pressure gradient and variation for different of A when $\Omega = 1, \mathrm{M} = 0.99, Gr = 0.5, m =$

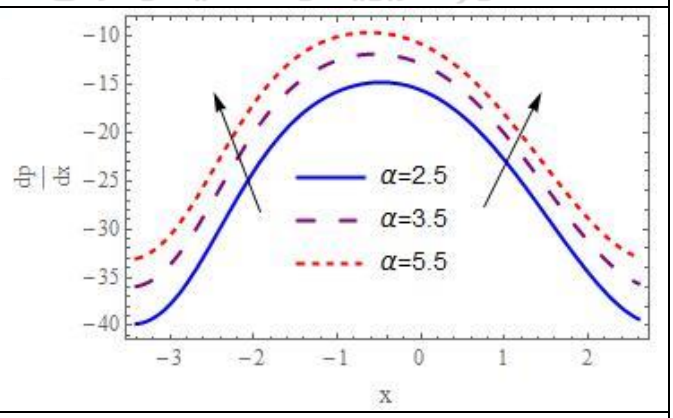

Figure 15: Pressure gradient and variation for different of α when $\Omega = 1, \mathrm{M} = 0.99, Gr = 0.5, m =$

JOBS
مجلة العلوم الأساسية
Journal of Basic Science
Print -ISSN 2306-5249
Online-ISSN 2791-3279
العدد السابع عشر
2023م /1444هـ

$0.05, \alpha = 2.5, \mathrm{Re} = 0.4, \mathrm{Fr} = 1, B = 1, \mathrm{Da} = 6, \phi = 2.4, \alpha 1 = 2.5$

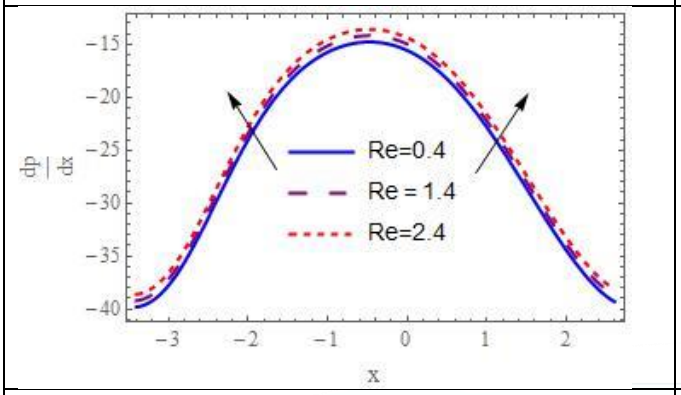

Figure 16: Pressure gradient and variation for different of Re when $\Omega = 1, \mathrm{M} = 0.99, Gr = 0.5, m = 0.05, A = 0.05, \alpha = 2.5, Fr = 1, B = 1, \mathrm{Da} = 6, \phi = 2.4, \alpha 1 = 2.5$

$0.05, A = 0.05, \mathrm{Re} = 0.4, \mathrm{Fr} = 1, B = 1, \mathrm{Da} = 6, \phi = 2.4, \alpha 1 = 2.5$

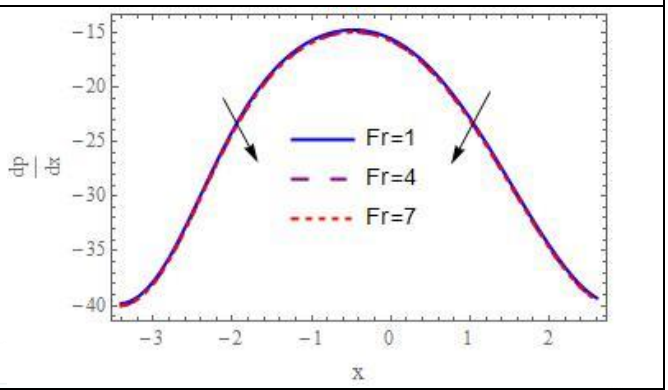

Figure 17: Pressure gradient and variation for different of Fr when $\Omega = 1, \mathrm{M} = 0.99, Gr = 0.5, m = 0.05, A = 0.05, \alpha = 2.5, \mathrm{Re} = 0.4, B = 1, \mathrm{Da} = 6, \phi = 2.4, \alpha 1 = 2.5$

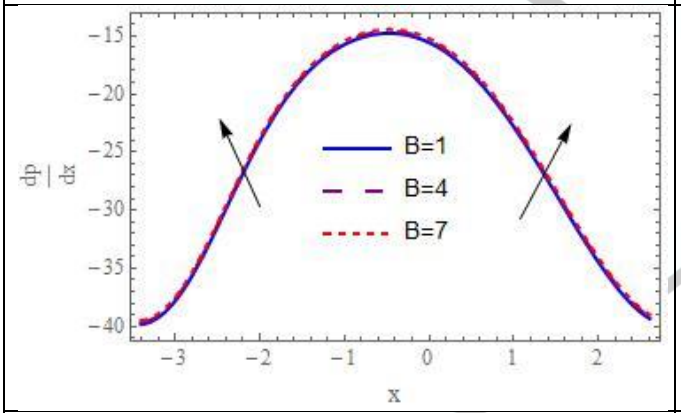

Figure 18: Pressure gradient and variation for different of B when $\Omega = 1, \mathrm{M} = 0.99, Gr = 0.5, m = 0.05, A = 0.05, \alpha = 2.5, \mathrm{Re} = 0.4, \mathrm{Fr} = 1, \mathrm{Da} = 6, \phi = 2.4, \alpha 1 = 2.5$

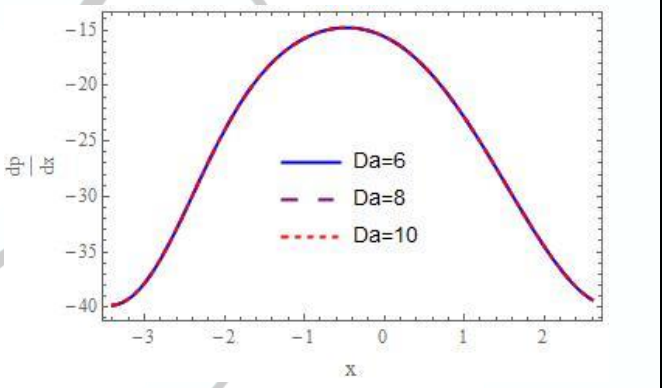

Figure 19: Pressure gradient and variation for different of Da when $\Omega = 1, \mathrm{M} = 0.99, Gr = 0.5, m = 0.05, A = 0.05, \alpha = 2.5, \mathrm{Re} = 0.4, \mathrm{Fr} = 1, \mathrm{B} = 1, \phi = 2.4, \alpha 1 = 2.5$

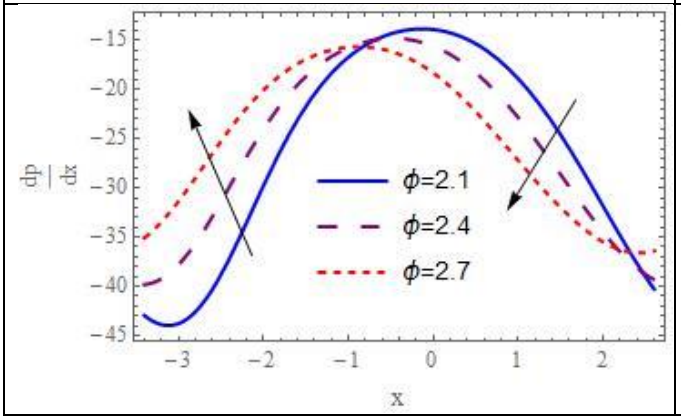

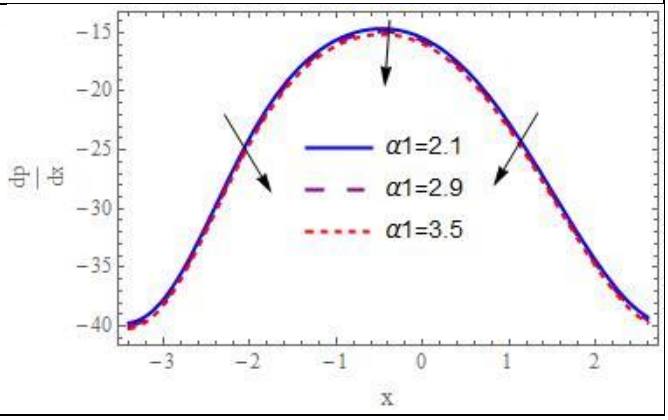

JOBS مجلة العلوم الأساسية
Journal of Basic Science
Print -ISSN 2306-5249
Online-ISSN 2791-3279
العدد السابع عشر
2023م /1444هـ

Figure 20: Pressure gradient and variation for different of ϕ when $\Omega = 1, \mathrm{M} = 0.99, Gr = 0.5, m = 0.05, A = 0.05, \alpha = 2.5, \mathrm{Re} = 0.4, \mathrm{Fr} = 1, \mathrm{B} = 1, Da = 6, \alpha 1 = 2.5$	Figure 21: Pressure gradient and variation for different of $\alpha 1$ when $\Omega = 1, \mathrm{M} = 0.99, Gr = 0.5, m = 0.05, A = 0.05, \alpha = 2.5, \mathrm{Re} = 0.4, \mathrm{Fr} = 1, \mathrm{B} = 1, Da = 6, \phi = 2.4$

Conclusions:

In this article, the influence of heat transfer and rotation on a Sutterby fluid in an asymmetric channel was investigated. In this investigation, a lot of attention has been paid to the analysis of things like velocity distribution and pressure gradient based on a simple analytical solution. The key findings of the current research are summarized below:

❖ As (Ω), (M), (m), (α), (B) and (Da) goes up, the axial velocity has no effect.

❖ The axial velocity reduces near the left wall of the channel and near the right middle of the channel as (Gr) increases, while it rises near the right wall of the channel and near the left middle of the channel.

❖ The axial velocity is increased in the middle of the channel as (A) increases, whereas it decreases near the channel wall.

❖ As (ϕ) increases, the axial velocity decreases along the left side and the near right side of the channel while it increases near the right middle of the channel.

❖ As increasing (Ω), (M), (m) and (Da) has no effect in pressure gradient. Increasing (Gr) increases the pressure gradient along the channel.

❖ The pressure gradient rises in the middle of the channel while it decreases in near the channel wall as (A) increases.

❖ As raising (α) results increases in the pressure gradient. The pressure gradient increases with the increasing Reynold number (Re).

❖ As increasing (Fr) little decreases in the pressure gradient. As (B) goes up, the pressure gradient has little rise.

❖ The pressure gradient rises along the left wall as the face difference (ϕ) increases whereas reduce along the right side of the channel.

❖ The pressure gradient has little decreasing with increasing of ($\alpha 1$).

Declaration of the authors:

- Competing Interests: None.
- We hereby confirm that all the Figures included in the article are ours.
- Ethical Approval: The University of Baghdad's local ethics committee approved the study.

Author's contributions statement:

This work was carried out in collaboration between all authors. Asmaa A. Mohammed and Liqaa Zeki Hummady read and approved the final manuscript.

JOBS
مجلة العلوم الأساسية
Journal of Basic Science
Print -ISSN 2306-5249
Online-ISSN 2791-3279
العدد السابع عشر
2023م /1444هـ

References:

1. Abdulhadi, A. M., & Ahmed, T. S. (2017). Effect of magnetic field on peristaltic flow of Walters' B fluid through a porous medium in a tapered asymmetric channel. *Journal of Advances in Mathematics*, *1*(12), 6889–6893.

2. Abdulhussein, H., & Abdulhadi, A. M. (2022). Impact of Couple Stress and Rotation on Peristaltic Transport of a Powell-Eyring Fluid in an Inclined Asymmetric Channel with Hall and Joule Heating Hanaa. *Journal of Basic Science*, *8(13)*, 483–509: http://bsj.uowasit.edu.iq

3. Abdulla, S. A., & Hummady, L. Z. (2021). Inclined magnetic field and heat transfer of asymmetric and porous medium channel on hyperbolic tangent peristaltic flow. *International Journal of Nonlinear Analysis and Applications*, *12*(2), 2359–2373. https://doi.org/10.22075/ijnaa.2021.5382

4. Ahmad, S., Farooq, M., Javed, M., & Anjum, A. (2018). Double stratification effects in chemically reactive squeezed Sutterby fluid flow with thermal radiation and mixed convection. *Results in Physics*, *8*, 1250–1259.

5. Ali, H. A. (2022). Impact of Varying Viscosity with Hall Current on Peristaltic Flow of Viscoelastic Fluid Through Porous Medium in Irregular Microchannel. *Iraqi Journal of Science*, 1265–1276.

6. Alshareef, T. S. (2020). Impress of rotation and an inclined MHD on waveform motion of the non-Newtonian fluid through porous canal. *Journal of Physics: Conference Series*, *1591*(1), 12061.

7. Atlas, F., Javed, M., & Imran, N. (2020). Effects of heat and mass transfer on the peristaltic motion of Sutterby fluid in an inclined channel. *Multidiscipline Modeling in Materials and Structures*, *16*(6), 1357–1372.

8. El-Dabe, N. T. M., Moatimid, G. M., Mohamed, M. A. A., & Mohamed, Y. M. (2021). A couple stress of peristaltic motion of Sutterby micropolar nanofluid inside a symmetric channel with a strong magnetic field and Hall currents effect. *Archive of Applied Mechanics*, *91*(9), 3987–4010.

9. Hayat, T., Ayub, S., Alsaedi, A., Tanveer, A., & Ahmad, B. (2017). Numerical simulation for peristaltic activity of Sutterby fluid with modified Darcy's law. *Results in Physics*, *7*, 762–768.

10. Hayat, T., Nisar, Z., Alsaedi, A., & Ahmad, B. (2021). Analysis of activation energy and entropy generation in mixed convective peristaltic transport of Sutterby nanofluid. *Journal of Thermal Analysis and Calorimetry*, *143*(3), 1867–1880.

11. Hummady, L., & Abdulhadi, A. (2014). Influence of MHD on peristaltic flow of couple stress fluid through a porous medium with slip effect. *Advanced in Physics Theories Applications*, *30*.

12. Kalyani, K., & MVVNL, S. R. (2021). A Numerical Study on Cross Diffusion Cattaneo-Christov Impacts of MHD Micropolar Fluid Across a Paraboloid. *Iraqi Journal of Science*, 1238–1264.
13. Kareem, R. S., & Abdulhadi, A. M. (2020). Impacts of Heat and Mass Transfer on Magneto Hydrodynamic Peristaltic Flow Having Temperature-dependent Properties in an Inclined Channel Through Porous Media. *Iraqi Journal of Science*, 854–869.
14. Khudair, W. S., & Dwail, H. H. (2021). Studying the magnetohydrodynamics for williamson fluid with varying temperature and concentration in an inclined channel with variable viscosity. *Baghdad Science Journal*, *18*(3). https://doi.org/10.21123/BSJ.2021.18.3.0531
15. Latham, T. W. (1966). *Fluid motions in a peristaltic pump.* Massachusetts Institute of Technology.
16. Mohaisen, H. N., & Abedulhadi, A. M. (2022). Effects of the Rotation on the Mixed Convection Heat Transfer Analysis for the Peristaltic Transport of Viscoplastic Fluid in Asymmetric Channel. *Iraqi Journal of Science*, 1240–1257.
17. Nassief, A. M., & Murad, M. A. (2020). The influence of magnetohydrodynamic flow and slip condition on generalized Burgers' fluid with fractional derivative. *Baghdad Science Journal*, *17*(1). https://doi.org/10.21123/bsj.2020.17.1.0150
18. Ramesh, K., & Prakash, J. (2019). Thermal analysis for heat transfer enhancement in electroosmosis-modulated peristaltic transport of Sutterby nanofluids in a microfluidic vessel. *Journal of Thermal Analysis and Calorimetry*, *138*(2), 1311–1326.
19. Sadaf, H., Akbar, M. U., & Nadeem, S. (2018). Induced magnetic field analysis for the peristaltic transport of non-Newtonian nanofluid in an annulus. *Mathematics and Computers in Simulation*, *148*, 16–36.
20. Shapiro, A. H., Jaffrin, M. Y., & Weinberg, S. L. (1969). Peristaltic pumping with long wavelengths at low Reynolds number. *Journal of Fluid Mechanics*, *37*(4), 799–825.
21. Sutterby, J. L. (1966). Laminar converging flow of dilute polymer solutions in conical sections: Part I. Viscosity data, new viscosity model, tube flow solution. *American Institute of Chemical Engineers*, *12*(1), 63–68.